Association between MR Imaging Measurements and Image-Guided Tissue Histopathology in Patients with Recurrent GBM

Qiuting Wen[1,2], Adam Elkhaled[2], Emma Essock-Burns[1], Annette Molinaro[3], Joanna Phillips[3,4], Susan M. Chang[3], Soonmee Cha[3], and Sarah J. Nelson[1,5]

[1]Graduate Group in Bioengineering, UC Berkeley/UC San Francisco, San Francisco, CA, United States, [2]Department of Radiology and Biomedical Imaging, UC San Francisco, San Francisco, CA, United States, [3]Department of Neurological Surgery, UC San Francisco, San Francisco, CA, United States, [4]Department of Pathology, UC San Francisco, UCSF San Francisco, CA, United States, [5]Bioengineering and Therapeutic Science, UC San Francisco, San Francisco, CA, United States

Introduction: Treatment with radiation and chemotherapy may result in gliosis, edema and necrosis, which can mimic tumor recurrence in standard MR images. Differentiating between these effects is a critical central challenge in neuro-oncology [1]. Acquisition of image guided tissue samples can enable the association of pathological properties of the tissue with pre-surgical MR parameters [2]. *Ex vivo* spectroscopy also offers direct association of pathology with a wide range of cellular metabolites [3]. The purpose of this study was to evaluate which *in vivo* and *ex vivo* MR parameters were able to distinguish between tumor and treatment effect for patients with GBM.

Data Acquisition: 152 tissue samples were collected from 73 patients with an original diagnosis of GBM, who were undergoing surgical resection due to suspected recurrence. *In vivo* MR imaging was done pre-operatively using a 3T (or 1.5T) GE scanner. MR exams included anatomic imaging (axial FLAIR, FSE and pre- and post- contrast T1-weighted 3D IRSPGR), physiological imaging (6-directional DWI; dynamic susceptibility contrast (DSC) imaging) and proton spectroscopic imaging (lactate-edited 3D MRSI). The MR images were co-registered and resampled to be in the same orientation. Maps of the apparent diffusion coefficient (ADC), fractional anisotropy (FA) and three eigenvalues (ev1, ev2, ev3) were obtained from the DTI sequence. Maps of peak height (PH), recirculation factor (RF), and percent recovery to baseline (RECOV) were estimated from the DSC susceptibility curves. The amplitudes of peaks corresponding to choline (Cho), creatine (Cr), N-acetylaspartate (NAA), lactate (Lac), and lipid (Lip) were estimated from the MRSI data. One to four image-guided tissue samples (about 5mm-diameter, 50mg) were collected from regions that were suspicious for recurrent tumor based on *in vivo* MRI features. Samples were divided into two parts, one was fixed for histological analysis and the other frozen for analysis using high-resolution magic angle spinning (HRMAS) spectroscopy. The *ex vivo* HRMAS data were acquired at 11.7 T using a Varian INOVA spectrometer equipped with a gHX gradient nanoprobe. The data were then processed using jMRUI and a customized QUEST fitting algorithm to estimate metabolite concentrations.

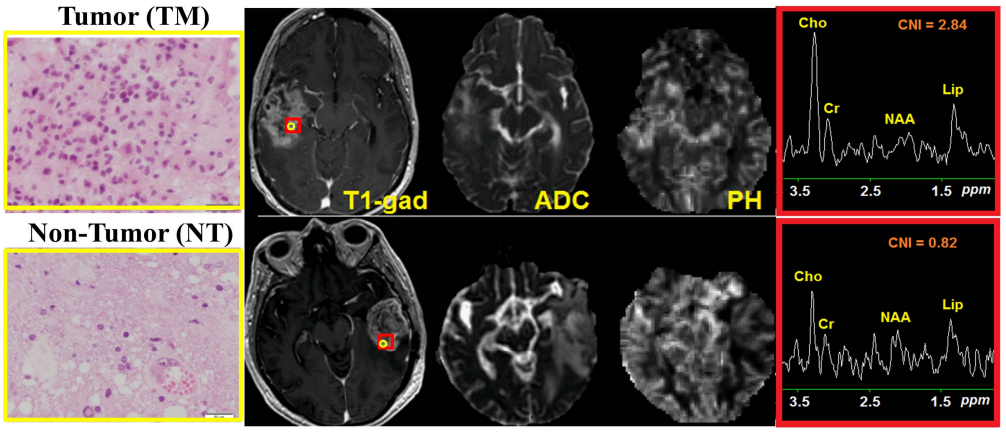

Figure 1. Pathologically confirmed tumor (TM) (upper) and non-tumor (NT) (lower) samples. From left to right: H&E staining, and *in vivo* MR imaging – T1-gad, ADC, PH and MRSI. On T1-gad image, yellow circle denotes the sample ROI, and red box represents MRSI voxel at the sample location.

Analysis: *MRI analysis*: Tissue coordinates were used to define spherical ROIs of 5mm in diameter. Median values of MRI parameters were therefore calculated within each ROIs. *Histopathology*: Tissue slides were given a tumor cellularity score ranging from 0~3 by a board certified pathologist based on the contribution of tumor cellularity to total cellularity. Samples with a tumor score of 0 were considered to be non-tumor (NT) and those with a score of 2 or 3 to be tumor (TM). Samples with a score of 1 were excluded to avoid ambiguity. *Statistical Analysis*: A generalized estimated equation (GEE) was performed to estimate the coefficient of each MRI variables and its associated categories (NT or TM). GEE accounts for the fact that multiple samples were taken from the same patient. Field strength and flip angles were adjusted for related parameters.

Results: Summary statistics for MRI values between the NT and TM groups are shown in Table 1. PH was found to be higher in the TM group ($p <$ .02). Both *in vivo* MRSI and *ex vivo* HRMAS showed significantly lower NAA in the TM group ($p <$.02 and $p <$.001 respectively). HRMAS also showed lower Cr in the TM group ($p <$.04). By only looking at samples acquired from contrast-enhancing lesions (CE), ADC was found to be lower ($p <$.05) and PH was higher ($p <$.04) in the TM group. *Ex vivo* NAA was also lower in the TM group ($p <$.02).

		Sequence	Parameter	P-val	Odds Ratio	Number of Samples		# Surgical Events
						TM	NT	
All Lesions	*in vivo MR*	DWI	*None*					
		DSC	PH	*0.013*	1.99	75	50	62
		MRSI	NAA	*0.013*	0.02	30	22	30
	ex vivo MR	HRMAS	NAA	*0.001*	3E-16	16	10	20
			CR	*0.037*	0.43	32	17	31
CE	*in vivo MR*	DWI	ADC	*0.041*	0.34	62	37	59
		DSC	PH	*0.036*	2.04	54	31	51
	ex vivo MR	HRMAS	NAA	*0.010*	8E-16	13	4	14

Table 1. Summary of MR parameters found to be significantly different between samples classified as TM and NT.

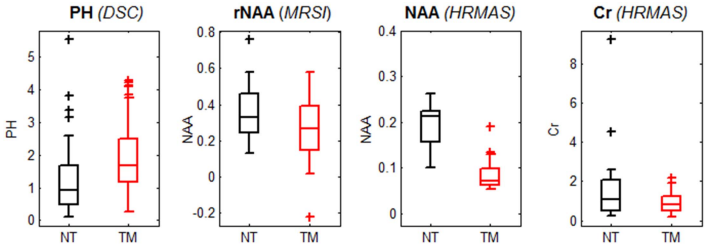

Figure 2. Box-plot of overall significant MR parameters in NT and TM groups.

Discussion: Our results showed the ability of PH, *in vivo* NAA, *ex vivo* NAA and Cr in differentiating tumor recurrence from treatment effect, which is consistent with the clinical findings that tumor recurrence has elevated angiogenesis and causes more neuronal disruption. It should be noted that there is overlap between the two groups for these parameters (see Figure 2), which suggests that future studies should consider using a multi-variate index to map out regions of recurrent tumor.

References: [1] Clarke JL, Chang S. Curr Neurol Neurosci Rep. 2009 May; 9(3):241-6. [2] Barajas RF Jr, Neuro Oncol. 2012 Jul; 14(7):942-54. [3] Srinivasan R. Neuro Oncol. 2010 November; 12(11): 1152–1161. **Acknowledgements:** Funding for these studies was provided by RO1 CA127612 and P01 CA118816.